The Circle Diagram in the Group Velocity Domain for Rossby Wave under the Horizontally Non-Uniform Flow

Yanjie Li[1], Jin Feng[2], Jianping Li[3, 4], and Sen Zhao[5, 6]

[1]*State Key Laboratory of Numerical Modeling for Atmospheric Sciences and Geophysical Fluid Dynamics, Institute of Atmospheric Physics, Chinese Academy of Sciences, Beijing, China*

[2]*Institute of Urban Meteorology, China Meteorological Administration, Beijing, China*

[3]*State Key Laboratory of Earth Surface Processes and Resource Ecology and College of Global Change and Earth System Science, Beijing Normal University, Beijing, China*

[4]*Laboratory for Regional Oceanography and Numerical Modeling, Qingdao National Laboratory for Marine Science and Technology, Qingdao, China*

[5]*School of Ocean and Earth Science and Technology, University of Hawaii at Mānoa, Honolulu, HI, USA*

[6]*Key Laboratory of Meteorological Disaster of Ministry of Education, and College of Atmospheric Science, Nanjing University of Information Science and Technology, Nanjing, China*

Abstract

Rossby wave propagation theory is reviewed under two kinds of non-uniform basic flows: the zonal mean (ZM) and horizontally non-uniform (HN) flows in this study. The diagrams in the wavenumber domain for stationary and non-stationary waves embedded in the ZM flow are given and discussed in comparison with previous studies. Then a circle diagram in the group velocity domain for waves embedded in the HN flow is derived from the formulas in forms of three vectors: the wavenumber, background wind and gradient of basic-state absolute velocity. Given the basic state, we can identify the maximum and minimum magnitude of group velocity and its departure from the background wind. These results provide insights into Rossby wave propagation behaviors in the real atmosphere.

(**Citation**: Li, Y. J., J. Feng, J. P. Li, and S. Zhao, 2018: The Circle diagram in the group velocity domain for Rossby wave under the horizontally non-uniform flow. *SOLA*, **14**, 121−125, doi: 10.2151/sola.2018-021.)

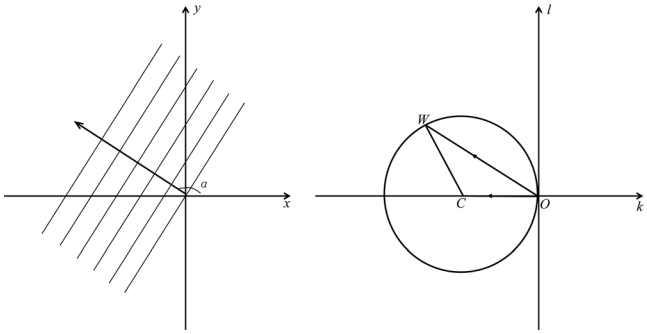

Fig. 1. Schematics for (a) a long-crested wave, slant lines are constant phase lines, and the arrow denotes the wavenumber vector, α denotes the angle between the arrow and the x-axis; and (b) the circle locus of the wavenumbers in (k, l) domain for free β-plane waves without the basic flow, following Fig. 1 in Longuet-Higgins (1964).

1. Introduction

Classical Rossby wave theory (Rossby 1939, 1945; Yeh 1949) is developed in the framework of the β-plane barotropic nondivergent vorticity model. However, this simplified framework neglects the spherical shape of the earth, as emphasized by Haurwitz (1940). Longuet-Higgins (1965) examined the validity of the β-plane approximation, and proved it to be of lower-order than the spheroidal approximation. Lindzen (1967) used two β-planes, one centered at the equator and the other at mid-latitudes, to simplify the spherical solution mathematically. Hoskins and Karoly (1981, herein referred to HK81) explored the Mercator projection to simplify the spherical vorticity equation, and derived its WKB solutions for disturbances embedded in a zonal mean (ZM) basic state. And many important properties derived from this theory match well with the observations on the atmospheric teleconnection. This motivate us to theoretically get knowledge on Rossby wave propagation in order to provide useful references for diagnosing and understanding the Rossby waves in the real atmosphere, and then further improve understandings on the climate variability resulted from these waves.

To demonstrate the properties of Rossby wave propagation, different diagrams are adopted to show the relations between wave parameters, including frequency, wavenumber, phase speed, and group velocity. Longuet-Higgins (1964) discussed the physical implications of these parameters in the wavenumber (k, l) domain. The wavenumber locus is a circle centered on $-\beta/2\omega$, 0 with the radius $\beta/2\omega$ (Fig. 1), where β is the meridional variation of the Coriolis parameter and ω is the angular frequency. In Fig. 1, $\overrightarrow{OW}$ denotes the wave number vector $\mathbf{K} = (k, l)$, and the phase velocity and group velocity are parallel to $\overrightarrow{OC}$ and $\overrightarrow{WC}$, respectively. Therefore, waves oriented toward the northwest will have group velocity toward the south, and waves oriented toward the southwest will have group velocity toward the north. This circle in Fig. 1 clearly expresses the relationships among the wavenumber, phase velocity, and group velocity. Duba and McKenzie (2012) showed circle and ellipse diagrams in phase velocity and group velocity domains, respectively. Their work emphasizes the variation of β in a simple basic flow. Classical textbooks (e.g. Pedlosky 1980, 2003) also show analogous diagrams in various forms to document Rossby wave propagation properties. However, these works are mostly for waves without or with a simple background environment.

Our previous studies on the wave propagation theory under the horizontally non-uniform (HN) flow (Li and Li 2012; Li et al. 2015; Zhao et al. 2015) suggest that their properties largely distinct from those under the ZM flow as discussed in HK81, especially in the tropical easterly. Here, we attempt to further discuss this theory to reveal a circle diagram in the group velocity domain. This work is organized as follow. Section 2 reviews the situation under the ZM flow, as in HK81 and Yang and Hoskins

Corresponding author: Jianping Li, Beijing Normal University, 19 Xin Jie Kou Wai Street, 1000875, Beijing, China. E-mail: ljp@bnu.edu.cn.

(1996) and shows diagrams in the wavenumber domain. Section 3 gives the fundamental theory in the HN flow and the diagram in the group velocity domain. Conclusions are given in Section 4.

2. Theory in the ZM flow

Following HK81, the dispersion relation for waves in the ZM flow $\bar{\psi}(\varphi)$ is in the form of

$$\omega = \bar{u}_M k - \frac{\beta_M k}{k^2 + l^2} \tag{1}$$

where ω is the angular frequency. k and l are the zonal and meridional wavenumber. $u_M = \bar{u}$ is the zonal background flow under the Mercator projectio

$$\beta_M = 2\Omega\cos^2\varphi/a - \partial/\partial y[1/\cos^2\varphi\partial/\partial y(\bar{u}_M\cos^2\varphi)] \tag{2}$$

is the meridional gradient of the basic-state absolute vorticity. φ is the latitude. Ω and a are the rotational frequency and radius of the earth, respectively. The phase speed along the x-axis c and group velocity $\mathbf{c}_g = (u_g, v_g)$ are derived as

$$c = \frac{\omega}{k} = \bar{u}_M - \frac{\beta_M}{k^2 + l^2}, \tag{3}$$

$$\mathbf{c}_g = (c, 0) + \frac{2\beta_M k}{(k^2 + l^2)^2}(k, l). \tag{4}$$

Comparing with the situation discussed by Longuet-Higgins (1964) in which waves are always non-stationary, the inclusion of the ZM basic flow allows for stationary waves with wavenumber satisfying

$$k^2 + l^2 = r^2, \tag{5}$$

$$\mathbf{c}_g = \frac{2\bar{u}_M k}{r^2}(k, l), \tag{6}$$

where $r = (\beta_M/\bar{u}_M)^{1/2}$. The locus of the wavenumber in the (k, l) domain is a circle centered at (0, 0) with a radius $\overrightarrow{OW}$ at the magnitude of r (shown as Fig. 2a). And the Eq. (6) suggests that the group velocity $\mathbf{c}_g$ for stationary wave is parallel to its wavenumber vector $\mathbf{K} = (k, l)$, which indicates that the stationary wave energy disperses normally to the constant phase lines. Therefore, stationary waves with a NE–SW tilted constant phase line ($kl < 0$) tend to propagate southward, while those oriented SE–NW ($kl > 0$) tend to propagate northward. And the zonal dispersion is always toward the east. These characteristics of wave shapes and propagation can be observed from previous barotropic model results

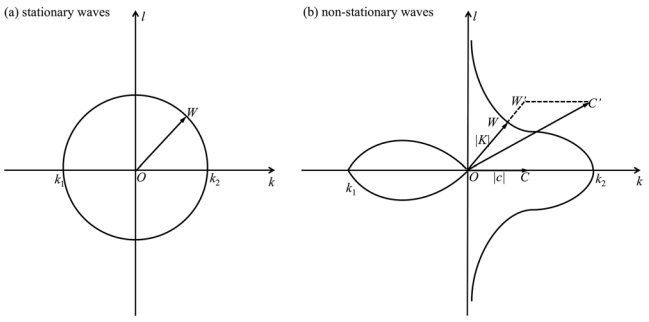

Fig. 2. Locus of the wavenumbers in (k, l) domain for (a) stationary waves and (b) non-stationary waves embedded in a zonal mean basic flow $\bar{u}_M$ greater than $u_e = -\frac{\omega^2}{4\beta_M}$. k_1 and k_2 denote the two solutions for k to Eq. (8) when $l = 0$, $\overrightarrow{OW}$ denotes the wavenumber vector, $\overrightarrow{OC}$ and $\overrightarrow{OC'}$ denote the phase velocity along the x-axis and group velocity separately.

(Hoskins et al. 1977; Branstator 1983; Noae et al. 1997).

To be noted, the above mathematical equations and geometrical map have limited valid range for wave propagation, which depends on the basic state and the wave scales or shapes. The circle diagram in the wavenumber domain for stationary waves shown in Fig. 2a is valid on the condition that $r^2 > 0$. It means that stationary waves can propagate only in the westerly flow given that β_M are positive (this assumption is used in this section). In the vicinity of the zero β_M, the magnitude of the radius and group velocity decreases to zero. And when k approaches to zero, l tend to approach to r, and the magnitude of $\mathbf{c}_g$ approaches to zero. In these situations, Fig. 2a is invalid.

As $\bar{u}_M$ approaches to zero, the radius of this circle in (k, l) domain tends to be infinity, which indicates that the waves are of extreme small scales. Their group velocity as defined by the Eq. (6) tends to be zero, which indicates that these waves cannot propagate at the latitude with the zero zonal background flow. This situation corresponds to the "critical latitude" in HK81. While when l approaches to zero and k approaches to r, the zonal group velocity u_g tends to be twice of $\bar{u}_M$, and the meridional group velocity v_g tends to be zero. This situation corresponds to the concept of "turning latitude" in HK81, at where a wave with positive l and v_g tends to be reflected into a wave with negative l and v_g, indicating the change in propagation direction.

The abovementioned meridional propagation properties of Rossby waves are vital in get the knowledge of tropical-extratropical interaction and have been discussed in previous studies (e.g., HK81; HA93; Naoe et al. 1997; Enomoto and Matsuda 1999). Comparing with the stationary wave, relative fewer studies discussed on the non-stationary waves. Karoly (1983) examined the ray trajectory for 50-day and 20-day period waves with easterly phase velocity, and suggested a westward propagation across the easterly wind for waves with higher phase speed. Yang and Hoskins (1996) deliberated the propagation behaviors of non-stationary waves in terms of the wave theory and barotropic model. We here provide the basic diagram in the wavenumber domain as a supplementary.

For non-stationary waves, the diagram in the wavenumber domain differs from a circle diagram for the stationary waves, since the dispersion relation for them is a cubic equation in k and a quadratic equation in l as

$$k^2 + l^2 = \frac{\beta_M}{\bar{u}_M - c}. \tag{7}$$

Given k, we have the real solutions of the meridional wavenumber in the form of

$$l = \pm\sqrt{\frac{\beta_M}{\bar{u}_M - c} - k^2}, \tag{8}$$

which requires that the quantity under the radical sign is positive. This means a restriction by the basic state on the changes of the zonal wavenumber k and the frequency to favor the meridional propagation. After mathematical deduction shown in the Supplementary, we derived the range of propagation wavenumber as a function of the frequency and the zonal flow speed as Yang and Hoskins (1996) did,

$$\begin{cases} (0 < k_c < k < k_2) \cup (k_1 < k < 0), & \text{if } \bar{u}_M > 0, \omega > 0 \\ (0 < k < k_2) \cup (k_1 < k < k_c < 0), & \text{if } \bar{u}_M > 0, \omega < 0 \\ (k_2 < k < k_c < 0) \cup (0 < k < k_1), & \text{if } u_e < \bar{u}_M < 0, \omega > 0 \\ (0 < k < k_2) \cup (0 < k_1 < k < k_c), & \text{if } u_e < \bar{u}_M < 0, \omega < 0 \\ k_c < k < 0, & \text{if } \bar{u}_M < u_e < 0, \omega > 0 \\ 0 < k < k_c, & \text{if } \bar{u}_M < u_e < 0, \omega < 0 \end{cases} \tag{9}$$

where

$$u_e = -\frac{\omega^2}{4\beta_M},\quad k_c = \frac{\omega}{\bar{u}_M},$$
$$k_1 = \frac{\omega - \sqrt{\omega^2 + 4\beta_M \bar{u}_M}}{2\bar{u}_M},\quad k_2 = \frac{\omega + \sqrt{\omega^2 + 4\beta_M \bar{u}_M}}{2\bar{u}_M}. \tag{10}$$

k_c corresponds to the critical latitude where $\bar{u}_M - c$ approaches to zero, while k_1 and k_2 correspond to the turning latitude where the meridional wavenumber tends to be zero. The Eq. (9) is correspondent to Fig. 2 in Yang and Hoskins, while differs in two places. One is that their work considered positive values of k, while both positive and negative are included here. The other that there is no waves with the positive frequency exist in the easterly region in their work, while this kind of waves could exist with zonal wavenumber in the range of (k_2, k_c) or (0, k_1). And following their work, we plotted an analogous schematic map for the propagation wavenumber (shown in the Supplementary). In short, it is implied that non-stationary waves with specified zonal scales may propagate meridionally in the easterly background wind, and waves with westward phase velocity are more likely to propagate across the tropical easterlies than those with eastward phase velocity. These results are in consistence with previous studies.

Based on the analysis on the Eq. (8), Fig. 2b shows the l–k schematic diagram for non-stationary waves for the situation with $\bar{u}_M > u_e$, which allows for k_1 and k_2 as real numbers. The curve is symmetric about the k-axis, and intersects with it at (k_1, 0), (k_2, 0), and (0, 0). For the same magnitude of k, we have $\frac{\beta_M}{\bar{u}_M - c_+} > \frac{\beta_M}{\bar{u}_M - c_-}$ in the westerly jet for the positive frequency. Therefore, we can deduce from the Eq. (8) that the eastward phase ~~pr2opagating~~ waves (with k positive) tend to have a smaller scale than the westward phase propagating waves (with k negative). Besides, Fig. 2b and Eq. (4) indicate that the group velocity ($\overrightarrow{OC'}$) is the sum of the phase velocity vector ($\overrightarrow{OC}$) and the vector parallel to the wavenumber vector ($\overrightarrow{OW'}$). This means that the waves oriented SE–NW with eastward (westward) phase velocity and those oriented NE–SW with westward (eastward) phase velocity will have a northward (southward) group velocity.

3. Theory in the HN flow

Following previous studies (Karoly 1983; Li and Nathan 1997; Li et al. 2015), the dispersion relation for waves under the HN flow $\bar{\psi}(\lambda,\varphi)$ can be written into both the scalar and vector forms as

$$\omega = \omega_{doppler} + \omega_{intrinsic} = \mathbf{A}\cdot\mathbf{K}, \tag{11}$$

where

$$\mathbf{A} = (A_x, A_y) = \mathbf{V}_M + \frac{\boldsymbol{z}\times\nabla\bar{q}}{|\mathbf{K}|^2}, \tag{12}$$

$$\omega_{doppler} = \mathbf{V}_M\cdot\mathbf{K} = \bar{u}_M k + \bar{v}_M l, \tag{13}$$

$$\omega_{intrinsic} = \frac{\boldsymbol{z}\times\nabla\bar{\boldsymbol{q}}}{|\mathbf{K}|^2}\cdot\mathbf{K} = \frac{\bar{q}_x l - \bar{q}_y k}{k^2 + l^2}, \tag{14}$$

$$\bar{q} = \nabla_M^2\bar{\psi}/\cos^2\varphi + 2\Omega\sin\varphi, \tag{15}$$

∇ is the gradient operator and $\mathbf{z}$ is the vertical unit vector. $\bar{q}$ is the basic-state absolute vorticity. $\bar{q}_x$ and $\bar{q}_y$ are the zonal and meridional gradient of $\bar{q}$. $\omega_{doppler}$ and $\omega_{intrinsic}$ denote the Doppler-shift frequency and the intrinsic frequency, respectively. The formal results from the advection of a spatial phase pattern $\mathbf{K}$ past a static observer, denoting the Doppler-shifting effect by both zonal and meridional components of the background wind. The latter is the frequency observed by a device travelling with the basic flow $\mathbf{V}_M = (\bar{u}_M, \bar{v}_M)$ (Bühler 2009), and it is determined by the wave's spatial structure and the gradient of the basic-state absolute vorticity.

Let α, η, and γ denote the angles of $\mathbf{K}$, $\nabla\bar{q}$, and $\mathbf{V}_M$ with respect to the x-axis, that is,

$$(k,l) = |\mathbf{K}|(\cos\alpha, \sin\alpha), \tag{16}$$

$$(\bar{q}_x, \bar{q}_y) = |\nabla\bar{q}|(\cos\eta, \sin\eta), \tag{17}$$

$$(\bar{u}_M, \bar{v}_M) = |\mathbf{V}_M|(\cos\gamma, \sin\gamma), \tag{18}$$

we can derive the phase velocity and group velocity from Eq. (11). The phase velocities that depict constant phase lines propagating along the x- and y-axes are

$$c_x = \frac{\omega}{k} = A_x + A_y\tan\alpha, \tag{19}$$

$$c_y = \frac{\omega}{l} = A_x\cot\alpha + A_y, \tag{20}$$

respectively. The phase velocity vector parallel to the wavenumber vector $\mathbf{K}$ is defined as

$$\overrightarrow{c_p} = \frac{\omega}{|\mathbf{K}|^2}|\mathbf{K}| = \left(A_x\frac{k}{|\mathbf{K}|} + A_y\frac{l}{|\mathbf{K}|}\right)\frac{\mathbf{K}}{|\mathbf{K}|}. \tag{17}$$

The group velocity is obtained into a different form from both Karoly (1983) and Li and Nathan (1997), that is

$$\mathbf{c}_g = (u_g, v_g) = \mathbf{V}_M + \hat{\mathbf{c}}_g, \tag{18}$$

$$\hat{\mathbf{c}}_g = \frac{|\nabla\bar{q}|}{|\mathbf{K}|^2}(\sin(\eta - 2\alpha), \cos(\eta - 2\alpha)). \tag{19}$$

Corresponding to the wave frequency, the first term of Eq. (18) denotes the explicit advection by the background flow, and the second is the intrinsic group velocity determined by both the magnitude ($|\nabla\bar{q}|$) and the orientations of the basic-state absolute vorticity gradient and the wavenumber vector (η and α). The difference between $\mathbf{c}_g$ and $\mathbf{V}_M$ denotes the intrinsic group velocity $\hat{\mathbf{c}}_g$. It can be inferred from this equation that the environment with a strong absolute-vorticity gradient favors a large-scale wave propagating away from the basic flow, while that with a weak absolute-vorticity gradient favors a higher wavenumber wave propagating along the background flow.

Further, we identify that the group velocity vector $\mathbf{c}_g$ in the group velocity domain must satisfy

$$(u_g - \bar{u}_M)^2 + (v_g - \bar{v}_M)^2 = R^2, \tag{20}$$

where $R = |\nabla\bar{q}|/|\mathbf{K}|^2$. This equation indicates a circle centered at the point ($\bar{u}_M$, $\bar{v}_M$) with a radius proportional to the basic-state absolute vorticity gradient $|\nabla\bar{q}|$ and the wavelength $|\mathbf{K}|$. This circle diagram is appropriate for both stationary and non-stationary waves. Figure 3 shows its schematic maps in terms of the magnitudes of $|\mathbf{V}_M|$ and R. Three situations may occur: the origin O is outside ($R < |\mathbf{V}_M|$), on ($R = |\mathbf{V}_M|$), or inside ($R > |\mathbf{V}_M|$) the circle. Approximately, these three situations are correspondent to waves embedded in the middle-latitude westerly jet that are with westward phase velocity, stationary and with eastward phase velocity respectively. This could be inferred from the wavenumber equation as

$$K^2 = \frac{|\nabla\bar{q}|}{|\mathbf{V}_M - c_x|}\frac{\sin(\eta - \alpha)}{\cos(\gamma - \alpha)}. \tag{21}$$

The geometry of the circle diagram provides insights into several particular propagation behaviors for Rossby waves. The propagation behaviors in Fig. 3a are discussed in detail, where $\overrightarrow{OA}$ denotes the basic wind vector $\mathbf{V}_M$, the terms C, D, E, and F indicate particular termini of $\mathbf{c}_g$. C', D', and F' are the other intersections of the diameter with the circle linked to C, D, and F. From Eq. (19), the angle between $\hat{\mathbf{c}}_g$ and the x-axis can be determined as

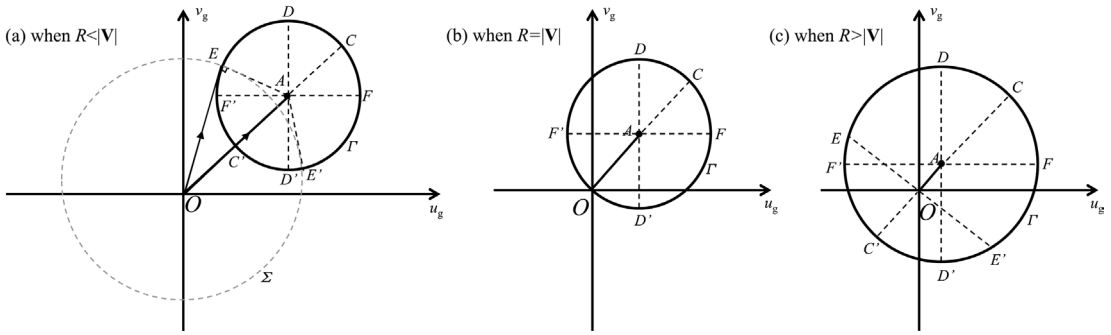

Fig. 3. Locus of group velocity **Γ** in (u_g, v_g) domain for waves embedded in the HN basic flow when the origin O (a) outside, (b) on, or (c) inside the circle. OA denotes the background wind vector, C, D, E, F denote special terminals of group velocity vector on the circle. E and E' in (a) are the two intersections between circle **Γ** (solid) and **Σ** (dashed, a circle centered at the origin O with the radius equal to the magnitude of $\overrightarrow{OE}$ and $\overrightarrow{OE'}$), while those in (c) are the two intersections between the circle **Γ** and the line which is perpendicular to $\overrightarrow{OA}$ and crossing the origin. Physical meanings are deliberated in the text.

$\frac{\pi}{2}+2\alpha-\eta$. Based on this, we can get several special wave energy dispersion properties as follow.

(1) For termini C and C', $\mathbf{c}_g$ is parallel to $\mathbf{V}_M$, and its maximum magnitude is $|\mathbf{V}_M| + R$ and minimum magnitude $|\mathbf{V}_M| - R$ is respectively. Correspondingly, the maximized group velocity $\overrightarrow{OC}$ and the minimized group velocity $\overrightarrow{OC'}$ departure from the x-axis at angles $\frac{1}{2}\left(\eta+\gamma-\frac{\pi}{2}\right)$ and $\frac{1}{2}\left(\eta+\gamma+\frac{\pi}{2}\right)$, respectively. Therefore, we can express the energy dispersion direction simply by the following rules: $\mathbf{c}_g$ is on the left side of $\mathbf{V}_M$ (when looking leeward) when $\eta+\gamma-\frac{\pi}{2}<2\alpha<\eta+\gamma+\frac{\pi}{2}$, and it is on the right side of $\mathbf{V}_M$ when $\eta+\gamma-\frac{3\pi}{2}<2\alpha<\eta+\gamma-\frac{\pi}{2}$.

(2) For termini E or E', $\mathbf{c}_g$ is perpendicular to $\hat{\mathbf{c}}_g$, and the ray trajectory lies to the left or right of the background wind vector, with maximum departure angles $2\alpha - \eta$ or $\eta - 2\alpha - \pi$ from the x-axis. The magnitude of $\mathbf{c}_g$ is given by the square root of $|\mathbf{V}_M|^2 + R^2$.

(3) For termini D or D', α equals $\eta/2$ or $(\pi + \eta)/2$, the zonal propagation is the same as the zonal flow, and the meridional propagation reaches a maximum relative to the meridional flow at a speed of R in the same or opposite direction.

(4) For termini F or F', α equals $(\eta - \pi/2)/2$ or $(\eta + \pi/2)/2$, the meridional propagation is the same as the meridional flow, and the zonal propagation relative to the zonal flow attains a maximum at a speed of R in the same or opposite direction.

The wave behaviors for termini C, D, and F (or C', D', and F') are the same in the other two situations with the origin O on (Fig. 3b) and inside (Fig. 3c) the circle. In Fig. 3c, E and E' denote wave energy propagation in the direction perpendicular to the background wind vector at a speed $\sqrt{R^2-|\mathbf{V}_M|^2}$.

Additionally, the Eqs. (11)−(20) can be simplified into the same form as those in the ZM flow. And the locus of the group velocity in (u_g, v_g) domain for waves in the ZM flow can also be derived as a circle in the similar way as a simplified Fig. 3. So, we don't give the details on it. We need to note that Fig. 2 is for waves under the ZM flow in the wavenumber (k, l) domain, while Fig. 3 is for waves under the HN flow in the group velocity (u_g, v_g) domain. We attempted to get the diagram for waves under the HN flow in the (k, l) domain, but it is found hard to derive a uniform diagram because there are more complex basic-state quantities determining wave shapes for the HN case than the ZM case.

4. Conclusion

In this study, we reexamine the basis of the two-dimensional Rossby wave theory following previous studies (Hoskins and Karoly 1981; Karoly 1983; HA 1993; Li and Nathan 1997; Li et al. 2015). Since wave properties closely depend on the basic state, two types of the non-uniform flows are considered as media for Rossby wave propagation: the ZM flow varying with latitude and the HN flow varying with both longitude and latitude.

Properties of stationary and non-stationary waves in the ZM flow are firstly reviewed, and schematic maps in the wavenumber domain for stationary and non-stationary waves are given under several assumptions respectively. And then relations between wave parameters (e.g., frequency, wavenumber, velocity) in the HN definition are highlighted. Karoly (1983) originally derived the formulas in the scalar forms. Li and Nathan (1997) discussed their vector forms. We here rewrite the phase velocity and group velocity formulas in terms of the magnitudes and angles of the wavenumber vector, the gradients of the basic-state absolute vorticity and the basic-state wind vector. A circle diagram for group velocity in the (u_g, v_g) domain is identified to depict the group velocity vector as a sum of the background wind vector and the intrinsic group velocity vector. Several special behaviors are identified from the circle diagram, including the maximum and minimum group velocity, the maximum departures from the background wind vector.

The two-dimensional wave propagation is viewed as the main mechanism of atmospheric wave train teleconnection (e.g. HK81, Trenberth et al. 1998). This study works on the fundamentals of the Rossby wave propagation theory, providing insights into the wave propagation properties. The circle diagram derived here shows us some special Rossby wave propagation behaviors. We can do further diagnosis based on them and track their propagation trajectories combining with the wave ray tracing method. These works are worthy to be deeply explored for their potential possibility of helping us to detect the Rossby wave signals in the real atmosphere. But, we need to keep in mind that there is limitation in the wave scales and validity of the diagrams shown in this work due to the nonuniform background flow in the consideration.

Acknowledgements

Authors are grateful for the comments by two anonymous reviewers. This work was jointly supported by the National Natural Science Foundation of China (NSFC) (projects 41575060 and 41790474), the SOA International Cooperation Program on Global Change and Air-Sea Interactions (GASI-IPOVAI-03).

Edited by: M. Yoshizaki

Supplement

Supplement includes the derivation of the Eq. (9).

References

Ambrizzi, T., B. J. Hoskins, and H. H. Hsu, 1995: Rossby wave propagation and teleconnection patterns in the austral winter. *J. Atmos. Sci.*, **52**, 3661−3672.

Branstator, G., 1983: Horizontal energy propagation in a barotropic atmosphere with meridional and zonal structure. *J. Atmos. Sci.*, **40**, 1689−1708.

Bühler, O., 2009: *Waves and mean flows*. Cambridge University Press, 341 pp.

Duba, C. T., and J. F. Mckenzie, 2012: Propagation properties of Rossby waves for latitudinal beta-plane variations of *f* and zonal variations of the shallow water speed. *Ann. Geophys.*, **30**, 849−855, doi:10.5194/angeo-30-849-2012.

Enomoto, T., and Y. Matsuda, 1999: Rossby wave packet propagation in a zonally varying basic flow. *Tellus A*, **51**: 588−602, doi:10.1034/j.1600-0870.1999.00004.x.

Haurwitz, B., 1940: The motion of atmospheric disturbances on the spherical Earth. *J. Mar. Res.*, **3**, 254−267.

Hoskins, B. J., A. J. Simmons, and D. G. Andrews, 1977: Energy dispersion in a barotropic atmosphere. *Quart. J. Roy. Meteor.*, **103**, 553−567.

Hoskins, B. J., and D. J. Karoly, 1981: The steady linear response of a spherical atmosphere to thermal and orographic forcing. *J. Atmos. Sci.*, **38**, 1179−1196.

Hoskins, B. J., and T. Ambrizzi, 1993: Rossby wave propagation on a realistic longitudinally varying flow. *J. Atmos. Sci.*, **50**, 1661−1661.

Karoly, D. J., 1983: Rossby wave propagation in a barotropic atmosphere. *Dyn. Atmos. Oceans*, **7**, 111−125.

Li, L., and T. R. Nathan, 1997: Effects of low-frequency tropical forcing on intraseasonal tropical-extratropical interactions. *J. Atmos. Sci.*, **54**, 332−346.

Li, Y. J., and J. Li, 2012: Propagation of planetary waves in the horizonal non-uniform basic flow. *Chinese J. Geophys.*, **55**, 361−371 (in Chinese).

Li, Y. J., J. Li, F. F. Jin, and S. Zhao, 2015: Interhemispheric propagation of stationary Rossby waves in the horizontally non-uniform background flow. *J. Atmos. Sci.*, **72**, 3233−3256.

Lindzen, R. D., 1967: Planetary Waves on Beta-Planes. *Mon. Wea. Rev.*, **95**, 441−451.

Longuet-Higgins, M., 1964: Planetary waves on a rotating sphere. *Proc. Roy. Soc.*, **279**, 446−473.

Longuet-Higgins, M., 1965: Planetary waves on a rotating sphere. II. *Proc. Roy. Soc.*, **284**, 40−68.

Naoe, H., Y. Matsuda, and H. Nakamura, 1997: Rossby wave propagation in idealized and realistic zonally varying flows. *J. Meteor. Soc. Japan*, **75**, 687−700.

Pedlosky, J., 1980: Geostrophical fluid dynamics. Springer-Verlag New York Inc., 624.

Pedlosky, J., 2003: *Waves in the ocean and atmosphere: introduction to wave dynamics*. Cambridge University Press, 260 pp.

Rossby, C.-G., 1939: Relations between variations in the intensity of the zonal circulation of the atmosphere and displacements of the semipermanent centers of action. *J. Mar. Res.*, **2**, 38−55.

Rossby, C. G., 1945: On the propagation of frequencies and energy in certain types of oceanic and atmospheric waves. *J. Atmos. Sci.*, **2**, 187−204.

Trenberth, K. E., G. W. Branstator, D. Karoly, A. Kumar, N.-C. Lau, and C. Ropelewski, 1998: Progress during TOGA in understanding and modeling global teleconnections associated with tropical sea surface temperatures. *J. Geophys. Res.*, **103**, 14291−14324.

Yang, G.-Y., and B. J. Hoskins, 1996: Propagation of Rossby waves of nonzero frequency. *J. Atmos. Sci.*, **53**, 2365−2378.

Yeh, T., 1949: On energy dispersion in the atmosphere. *J. Atmos. Sci.*, **6**, 1−16.

Zhao, S., J. Li, and Y. Li, 2015: Dynamics of an interhemispheric teleconnection across the critical latitude through a southerly duct during boreal winter. *J. Climate*, **28**, 7437−7456.

Manuscript received 21 February 2018, accepted 8 July 2018
SOLA: https://www.jstage.jst.go.jp/browse/sola/